NATURAL FREQUENCY OF GAS BUBBLE IN SLUG FLOW

Mazza, Ricardo A., mazza@fem.unicamp.br
Rosa, Eugênio S., erosa@fem.unicamp.
DE/FEM/UNICAMP – Caixa Postal 6122 - 13083-970 – Campinas – SP - Brazil

Abstract. *The slug flow is characterized by the succession of liquid pistons and long gas bubbles which are neither periodic in time nor in space. The gas content transported by the long bubble gives a compressibility to the gas-liquid mixture which, in the presence of liquid velocity disturbances, behave as a non-linear oscillator. The objective of this work is to study the oscillatory behavior of a single long gas bubble flowing between two liquid slugs disclosing the amplitude, phase and natural frequency. The analysis applies slug tracking physical model to describe the bubble to liquid slug interaction. The model solution is obtained using a numerical and analytical procedure. The former one is considered complete and embodies all non-linear terms of the physical model. The last one is an approximated solution given by a linearized version of the physical model. An analytical expression for the natural frequency in terms of the slug flow parameters is presented within the limit of validity of the linear domain.*

Keywords*: slug flow, natural frequency, slug tracking, oscillations*

1. INTRODUCTION

In laboratory conditions the slug flow is formed by continuous mixing of gas with liquid streams at the pipe inlet. Downstream the mixer the flow pattern is mostly described as a churn flow which eventually evolves to the slug flow pattern further downstream the mixer. Pressure fluctuations are developed during the process of mixing, propagate through out the line and induce oscillations into the liquid slugs and gas bubbles as they travel along the pipe. It is not clear yet if the induced gas bubble oscillations lead to bubble coalescence but certainly it is a mechanism which must be investigated. This motivation arises from similar studies with induced oscillations in spherical bubbles. The natural frequency and the vibration modes of spherical bubbles are described by the Rayleigh-Plesset equation, Leighton (1994) and Swift (2002). Also, it is generally recognized that the spherical bubble coalescence, in acoustically driven liquids, is mainly governed by interaction forces exerted by bubbles in response to the imposed acoustic field.

The oscillations of gas bubbles occurring in slug flow are still a new subject. Liang and Ma (2004) employ a mechanical oscillator analogy to describe the pressure and velocity oscillations happening in slug flow inside capillary tubes. Also Vergniolle and Brandeis (1996), Vergniolle et al. (1996) and James et al. (2004) studying the rising of a single gas bubbles in volcano lava channel propose an analytical expression for the natural frequency of bubble oscillation and a experimental set up in lab-scale to measure it. A straight forward transposition of these findings to the slug flow applied to the oil industry is not obvious. Nonetheless the gas bubble in slug flow, similarly to the study of induced oscillations in spherical bubbles, bear an analogy with mechanical oscillator where the spring constant is represented by the gas compressibility while the mass and the damping coefficient are represented by the slug mass and the wall friction. Due to the existence of several liquid pistons followed by gas bubbles flowing simultaneously inside a pipe the analysis becomes complex since we have several oscillators in series and the coupling between neighbors is not linear.

The oscillation phenomenon in multiple gas bubbles occurring in a slug flow is too complex to a first approach to this problem. It was decided to study a simpler case in which we are interested in the response of a single bubble to the impulse function in terms of its natural frequency, amplitude and phase. The knowledge of a single bubble natural frequency is still relevant to the study of multiple bubbles to give us a solid basis in terms of the physics of the phenomena to move to the complex case. The case study is described in Figure 1 as a single bubble with length L_B comprised by two non-aerated liquid slugs with lengths and velocities of L_{S0}, U_0 and L_{S1}, U_1, respectively. The pipe length is L and its diameter is D. The bubble front and tail are represented by the coordinates Y_1 and X_0, respectively. The oscillating phenomenon is studied numerically employing the slug tracking model and also analytically by linearizing the transport equations.
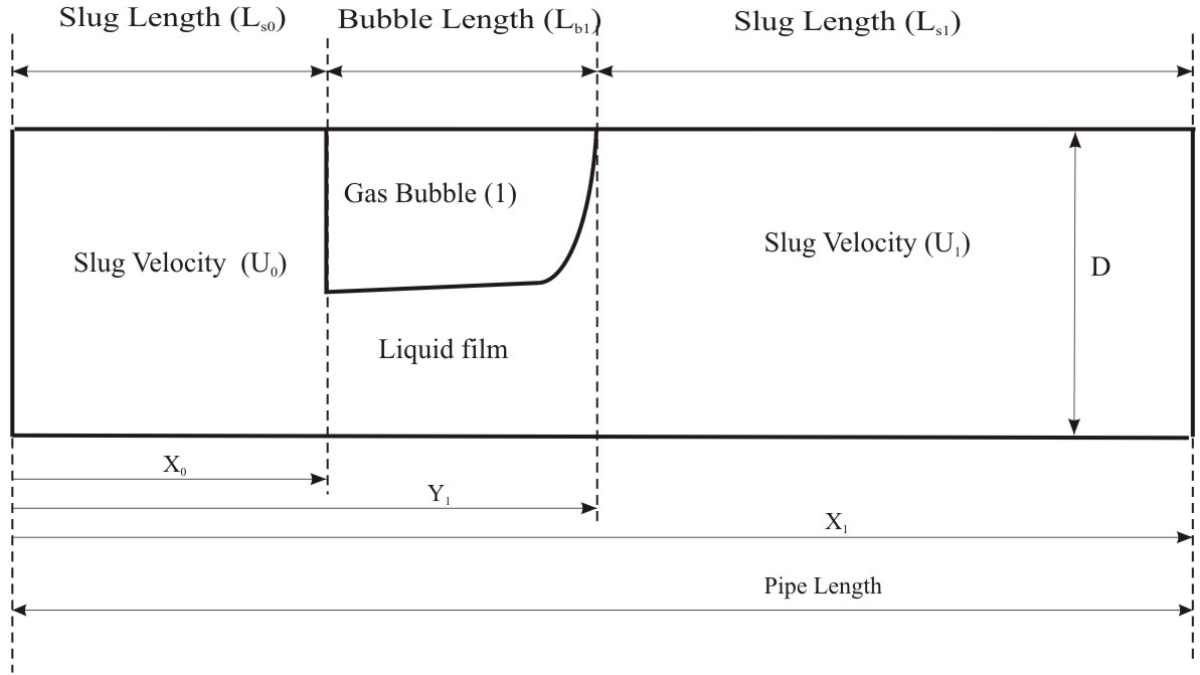
Figure 1 – Schematic diagram of the gas bubble inside the pipe and the used nomenclature.

2. PHYSICAL MODEL

The coupling between the gas bubble and the liquid slug is expressed by the gas conservation equation and liquid momentum, Eqs. (1) and (2):

$$U_1 = U_0 - \frac{L_{B1}\overline{R}_{G1}}{H_1}\frac{dH_1}{dt},$$ (1)

$$H_1 = H_{atm} + L_{S1}\frac{dU_1}{dt},$$ (2)

where U, L_{B1} and L_{S1} are as defined in Figure 1, H_1 and H_{atm} is the bubble and outlet pressure and density ratio, respectively, and R_{G1} is the gas volumetric fraction within the pipe volume taken by the gas bubble, shortly known as the bubble void fraction. The set of equations links the velocity difference of the liquid slugs with the time rate of the pressure and also the pressure difference with the acceleration of the liquid slug ahead of the gas bubble. The equations describe the displacement and velocity of the gas bubble and of the non-aerated liquid slug for a horizontal, isothermal and frictionless flow. Equations (1) and (2) are continuous in time but condensed in space, nonetheless they represent a hyperbolic system which carries the U and P information along characteristic lines defined by the bubble nose velocity. These equations constitute the basis of the slug tracking model shown in Franklin (2004) and Grenier (1997). For simplicity, it is used the ideal gas law for the state equation for the gas component.

The gas bubble oscillation study is based on the model output described by Eqs. (1) and (2). The initial condition is a steady flow state with the liquid slugs ahead and behind the gas bubble having the same velocities, $U_0 = U_1$. Since the flow is frictionless the outlet pressure prevails along the pipe, therefore the bubble pressure is also H_{atm}. At a time $t_0 > 0$, the velocity of the liquid slug behind the gas bubble, U_0, is disturbed for an instant and then returned to its initial value. The bubble oscillation analysis starts just after ceasing the velocity disturbance. Equations (1) and (2) are solved employing a numerical technique as shown in section 2.1 as well as analytically by linearizing the equation set as described in section 2.2.

2.1. Numerical Method

The set of equations (1) and (2) is discretized using the Crank Nicholson method ($\alpha = 0.5$) accordingly to Eq.(3) and is readily integrated in time.

$$\begin{bmatrix} \dfrac{1}{\alpha} \dfrac{L_{B1}^{O} \bar{R}_{G1}}{H_{1} \Delta t} & 1 \\[2ex] -1 & \dfrac{1}{\alpha}\left(\dfrac{L_{S1}^{O}}{\Delta t} \right) \end{bmatrix} x \begin{bmatrix} H_{1}^{N} \\[2ex] U_{1}^{N} \end{bmatrix} = \begin{bmatrix} \dfrac{1}{\alpha} \dfrac{L_{B1}^{O} \bar{R}_{G1}}{\Delta t} + U_{0}^{N} - \left(\dfrac{1-\alpha}{\alpha} \right)\left(U_{1}^{O} - U_{0}^{O} \right) \\[2ex] \dfrac{1}{\alpha} \dfrac{L_{S1}^{O} U_{1}^{O}}{\Delta t} - H_{atm} - \left(\dfrac{1-\alpha}{\alpha} \right)\left(H_{atm} - H_{1}^{O} \right) \end{bmatrix} , \tag{3}$$

where the super-indexes O and N represent, respectively, the previous and actual time and Δt is the time step and H is the ratio between the pressure and liquid density ($H=P/\rho_L$). As an implicit method it is intrinsically stable but, to ensure result with numerical accuracy it is necessary to enforce a Courant number less than 10^{-3}.

It is necessary to know the bubble length and bubble velocity to advance in time the numerical solution of the Eq. (3). The bubble length is determined enforcing the gas mass, within the bubble, to be constant in time and space:

$$L_{B1}^{N} = \frac{H_{1}^{O}}{H_{1}^{N}} \left(Y_{1}^{N} - X_{1}^{O} \right), \tag{4}$$

where X and Y are the coordinates describing, respectively, the liquid piston front and the gas bubble front as shown in Figure 1. The bubble front advance in space accordingly to the product of the bubble nose velocity with the time step:

$$Y_{1}^{N} = Y_{1}^{O} + V_{B} \Delta t , \tag{5}$$

where V_B is the bubble front velocity given by the kinematical relation proposed by Nicklin et. al (1962):

$$V_{B} = C_{0} U_{1} + V_{0} , \tag{6}$$

where C_0 e V_0 are constants which, accordingly to Bendiksen (1984), are:

$$\begin{cases} C_0 = 1.0 & e & V_0 = 0.54\sqrt{gD} & \text{for} & Fr < 3.5 \\ C_0 = 1.2 & e & V_0 = 0 & \text{for} & Fr > 3.5 \end{cases}, \tag{7}$$

and Fr is the Froude number based on the velocity of the liquid slug ahead of the bubble: $Fr = U_1 / \sqrt{gD}$.

The initial conditions have the liquid slugs traveling with the same speed, $U_0 = U_1$ and the bubble front traveling accordingly to Eq. (6) . The slugs and bubble velocities remain constant until a disturbance is applied in U_0. The disturbance is characterized rectangular pulse with width of Δt_d in time and height of 'a'. During the disturbance the liquid slug velocity is suddenly raised to $U_0 + a$, after ceasing the disturbance it attains its initial value, U_0. The frequency, phase and amplitude of the pressure and velocity signals are analyzed employing Fast Fourier Transform (FFT) algorithm. Equations (3) to (7) plus the signal analysis are assembled in a program developed to this application using Compaq Visual Fortran compiler.

2.2. Analytical Method

The set of equations (1) and (2) is not linear if we recognize that L_B, L_S change as the bubble oscillates in time or its front advances in space. An analytical solution for the equation system is sought by means of an approximate through linearization techniques. Considering that the velocity disturbance in U_0 will cause a periodic disturbance on U_1 and P_1, and then it is possible to express the instantaneous values as a sum of mean value plus its fluctuation. In this case the instantaneous values of L_B, U, L_S and P are represented by:

$$L_B = \bar{L}_B + \tilde{L}_B , \ U = \bar{U} + \tilde{U} , \ L_S = \bar{L}_S + \tilde{L}_S \text{ and } H = \bar{H} + \tilde{H} \tag{8}$$

where the super-scritp '−' means the averaged term and '~' its fluctuation. Equation (8) neglects the changes in R_G during the bubble oscillation. Substituting Eq.(8) in Eqs. (1) and (2) we have:

$$\bar{U}_1 + \tilde{U}_1 = \bar{U}_0 + \tilde{U}_0 - \frac{\left(\bar{L}_{B1} + \tilde{L}_{B1} \right) \bar{R}_{G1}}{\left(\bar{H}_1 + \tilde{H}_1 \right)} \frac{d\left(\bar{H}_1 \right)}{dt} - \frac{\left(\bar{L}_{B1} + \tilde{L}_{B1} \right) \bar{R}_{Gj}}{\left(\bar{H}_1 + \tilde{H}_1 \right)} \frac{d\left(\tilde{H}_1 \right)}{dt} , \tag{9}$$

$$\bar{H}_I + \tilde{H}_I = H_{atm} + \left(\bar{L}_{SI} + \tilde{L}_{SI}\right)\frac{d\bar{U}_I}{dt} + \left(\bar{L}_{SI} + \tilde{L}_{SI}\right)\frac{d\tilde{U}_I}{dt} . \tag{10}$$

After ceasing the disturbance the inlet velocity is equal to the outlet velocity, therefore:

$$\bar{U}_I = \bar{U}_0 , \tag{11}$$

furthermore, since $\bar{U}_0$ does not change in time so does $\bar{U}_I$, then:

$$\frac{d\bar{U}_0}{dt} = \frac{d\bar{U}_I}{dt} = 0 . \tag{12}$$

At last, since we are using a frictionless model, $\bar{H}_I$ does not change in time or in space so:

$$\frac{d\bar{H}_I}{dt} = 0 \text{ and } \bar{H}_I = H_{atm} . \tag{13}$$

Replacing Eqs. (11) to (13) into Eqs. (9) and (10), we find the equation set for the fluctuating components of $\tilde{P}_I$ and $\tilde{U}_I$:

$$\tilde{U}_I = \tilde{U}_0 - \frac{\left(\bar{L}_{BI} + \tilde{L}_{BI}\right)\bar{R}_{GI}}{\left(\bar{H}_I + \tilde{H}_I\right)}\frac{d\left(\tilde{H}_I\right)}{dt} , \tag{14}$$

$$\tilde{H}_I = \left(\bar{L}_{SI} + \tilde{L}_{SI}\right)\frac{d\tilde{U}_I}{dt} . \tag{15}$$

The coefficients multiplying the derivatives depend on the averaged plus fluctuating components of L_B, L_S and P. If we consider small disturbances in such way that $\tilde{L}_{BI}/\bar{L}_{BI} \ll 1$; $\tilde{L}_{SI}/\bar{L}_{SI} \ll 1$ and $\tilde{H}_{BI}/\bar{H}_{BI} \ll 1$ then we can approximate the instantaneous values by the averaged values:

$$\bar{L}_{BI} + \tilde{L}_{BI} \sim \bar{L}_{BI} , \tag{16}$$

$$\bar{L}_{SI} + \tilde{L}_{SI} \sim \bar{L}_{SI} , \tag{17}$$

$$\bar{H}_I + \tilde{H}_I \sim \bar{H}_I = H_{atm} . \tag{18}$$

Substituting Eqs. (16) thru (18) into Eqs. (14) and (15), we have the reduced form for the fluctuating components equations:

$$\tilde{U}_I = \tilde{U}_0 - \frac{\bar{L}_{BI}\bar{R}_{GI}}{H_{atm}}\frac{d\left(\tilde{H}_I\right)}{dt} , \tag{19}$$

$$\tilde{H}_I = \bar{L}_{SI}\frac{d\tilde{U}_I}{dt} . \tag{20}$$

The first order system of ODEs can be represented as a second order ODE substituting Eq. (19) into Eq.(20):

$$\frac{d^2\left(\tilde{H}_I\right)}{dt^2} + \frac{H_{atm}}{\bar{L}_{BI}\bar{R}_{GI}\bar{L}_{SI}}\tilde{H}_I = \frac{H_{atm}}{\bar{L}_{BI}\bar{R}_{GI}}\left(\frac{d\tilde{U}_0}{dt}\right) . \tag{21}$$

Equation (21) represents the fluctuating pressure equation with a forcing term given by the first order derivative of $\tilde{U}_0$ representing the velocity disturbance given by the Dirac Delta:

$$\tilde{U}_0 = V\delta\left(t - t_0\right),$$

(22)

where the constant V is defined by the product of the height by the width of the numerical pulse, $V = a.\Delta t_d$. The second order ODE, Eq.(21), has variable coefficients since $\overline{L}_{S1}$ changes with time as $\overline{L}_{S1} = L_{S1_{ini}} - V_B \cdot t$. Although, if we consider a slow change in time of $\overline{L}_{S1}$ in such way that:

$$\frac{V_B}{\overline{L}_{S1}} << \omega_0 \,,$$

(23)

where ω_0 is the natural frequency, we can further approximate Eq. (21) to a ODE with constant coefficients. The analytical solution comes from Laplace transform. The fluctuating pressure is:

$$\tilde{H}\left(t\right) = \begin{cases} 0 & \text{for} \quad t < t_0 \\ \dfrac{H_{atm}}{\overline{L}_{B1}\overline{R}_{G1}} V Cos\left(2\pi\omega_0\left(t - t_0\right)\right) & \text{for} \quad t \ge t_0 \end{cases}$$

(24)

and the natural frequency ω_0 arises from the homogenous part f Eq.(21) :

$$\omega_0 = \frac{1}{2\pi}\sqrt{\frac{H_{atm}}{\overline{L}_{B1}\overline{R}_{G1}\overline{L}_{S1}}} \;.$$

(25)

Substituting the definition of the fluctuating pressure, Eq. (24) into Eq. (19) we get the liquid slug velocity fluctuation:

$$\tilde{U}\left(t\right) = \begin{cases} 0 & \text{for} \quad t < t_0 \\ V\sqrt{\dfrac{H_{atm}}{\overline{L}_{B1}\overline{R}_{G1}\overline{L}_{S1}}} Sin\left(2\pi\omega_0\left(t - t_0\right)\right) & \text{for} \quad t \ge t_0 \end{cases}.$$

(26)

3. RESULTS

The study of the frequency, phase and amplitude of the pressure and velocity fluctuations P_1 and U_1 starts with the comparison of the numerical and analytical solution. This comparison is based on a test case with water flowing in a pipe with 26.5 mm in diameter and 20 m long with its outlet open to the atmosphere, $P_{out} = 100$ kPa. The pipe has an air bubble with void fraction of $R_G = 0.7$ and length $L_B = 0.8$ m with noise placed at $Y = 1.2$ m from the pipe inlet. The slug length at time begin was $L_{S1} = 18.8$ m. The initial velocities are $U_0 = U_1 = 0.5$ m/s and the velocity disturbance is set at 1s after the start up. The U_0 disturbance is shown in having a height of 0.1 m/s and a width of 0.2 s. The time series of the ratio between the instantaneous to the averaged value of P, U_0 and U_1 are shown in Figure 2.a. The extra 'x' axis on the figure represents the length of the liquid piston ahead of the bubble nose. The slug length ahead of the bubble and the time are related by the bubble nose traveling velocity, Eq. (6). The bubble pressure and the liquid piston velocity start oscillating after the disturbance with no damping on the amplitude due to the frictionless assumption. The pressure and velocity lags of a 90 degree phase. Also the fluctuating amplitude of the pressure and velocity are of 3% and 12%, respectively, of the averaged values. Figure 2.b exhibits the analytical solution evaluated at the same conditions and having the constant V in Eq. (22) determined by the product of the velocity disturbance height and width defined before, $V = 0.01$ m/s. As seen in Figure 2.b, the pressure and velocity also lags of a 90 degree phase due to the character of the Cos and Sin functions embodied in Eqs. (24) and (26). The amplitudes of the fluctuating components of pressure and velocity are, respectively, of: 2.5% and 7% which values comparable to the numerical estimates.
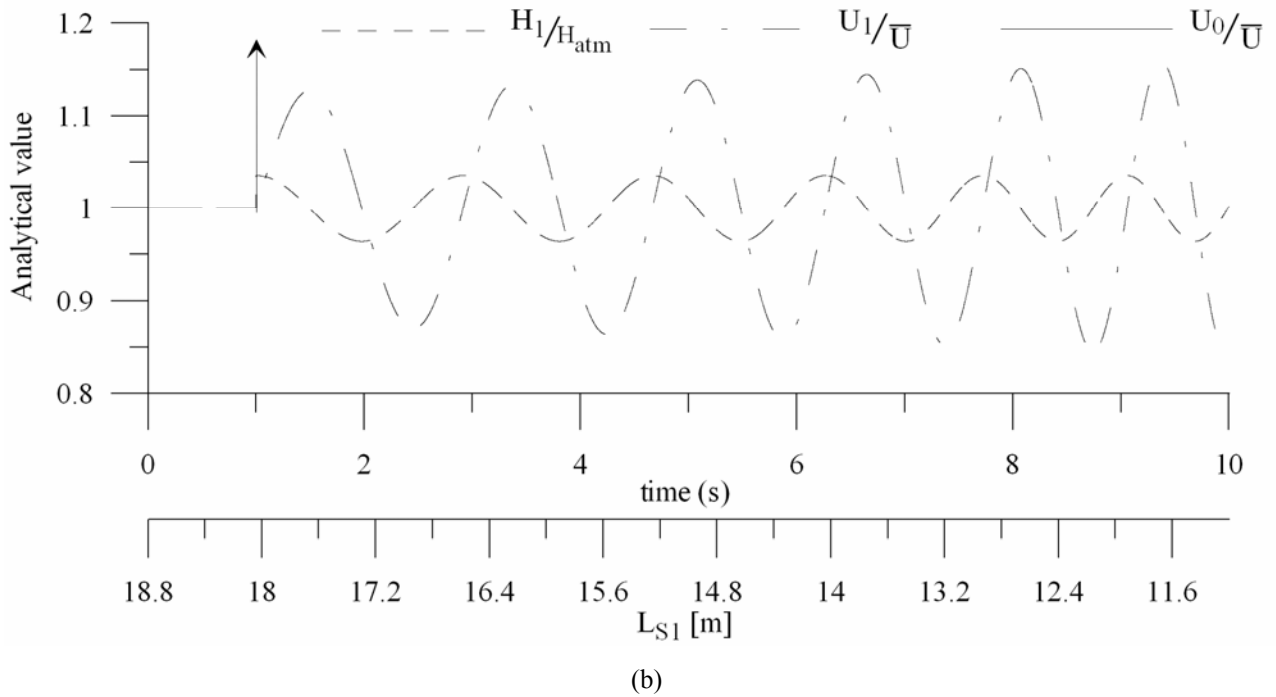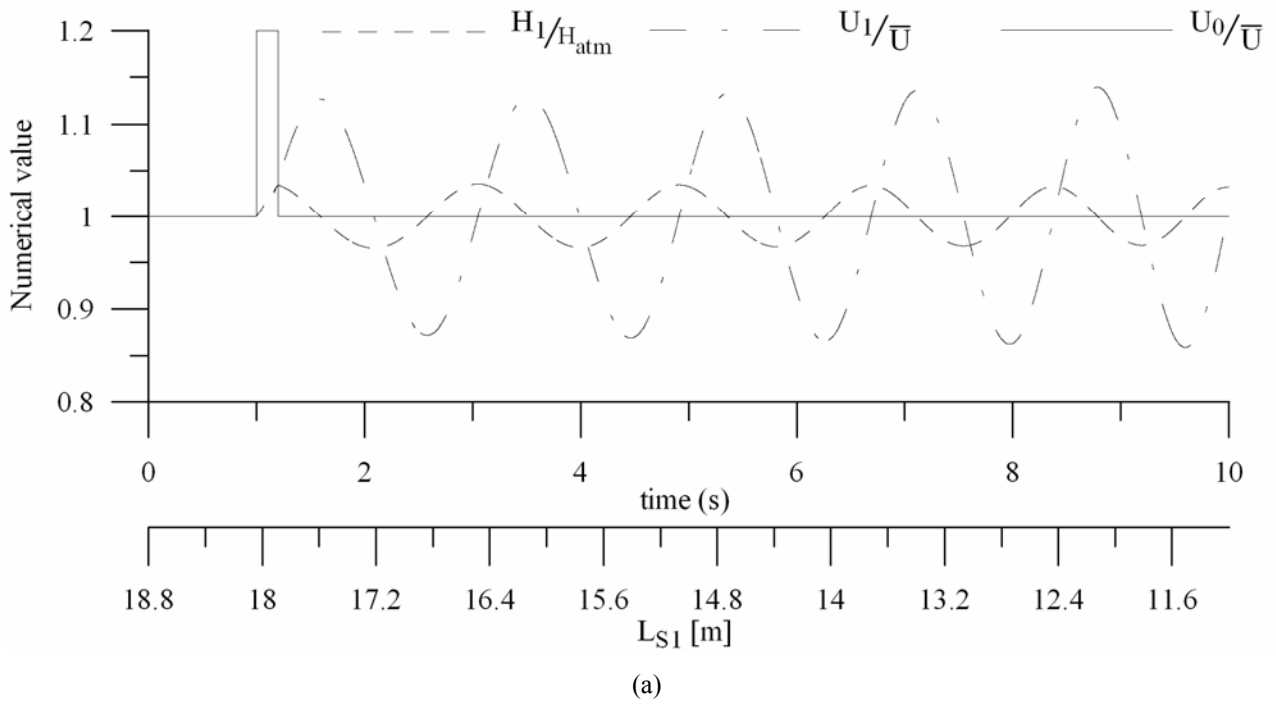
(a)

(b)

Figure 2 – Instantaneous to averaged ratio of H_1, U_1 and U_0 as a function of time or length of the liquid piston ahead of the bubble nose. Inlet conditions defined in the test case: (a) numerical results; (b) analytical results.

The natural frequency is one of the most relevant information of this work. It was disclosed in an analytical expression, Eq. (25), based on an the approximate analysis developed on section 2.2. The square of the natural frequency is directly proportional to the bubble pressure and inversely proportional to the liquid density, bubble void fraction, bubble length and the liquid slug length ahead of the bubble nose. Since Eq. (21) was approximated by an ODE with constant coefficients a straight forward analogy with the mechanical oscillator can be drawn. Recognizing

the natural frequency of a mechanical oscillator is defined by $\omega_0 = \dfrac{1}{2\pi}\sqrt{\dfrac{k}{m}}$ where k and m represent the spring constant

and the mass, respectively. It is possible to define the analog to the spring constant to the mass of the oscillator in terms of the properties of the slug flow by comparing this definition of natural frequency with the one given by Eq. (25):

$$k = \frac{P_{atm} A_T}{L_{B1} \cdot R_{G1} \cdot \rho_L} \quad \text{and} \quad m = \rho_L A_T L_{S1}. \tag{27}$$

The spring stiffness increases with the increase of the gas pressure or with the decrease of the bubble length and void fraction. The mass of the system is the mass of liquid ahead of the bubble nose.

The natural frequency expression is valid as long Eq. (23) is true or, introducing the parameter ε:

$$\varepsilon = \sqrt{\frac{P_{atm}}{R_G \cdot \rho_L \cdot V_B^2} \cdot \frac{L_{S1}}{L_{B1}}} \gg 1. \tag{28}$$

A comparison of the numerical and analytical estimates of the natural frequency for the given conditions on the test case is done in Figure 3 as a function of the parameter ε defined in Eq. (28). The changes during the test case are due to the changes on L_S because the bubble traveled along the pipe thus diminishing the liquid slug ahead of it. As seen on Figure 3 the analytical solution approaches asymptotically the numerical solution as ε increases. Complementary, as length of the liquid slug ahead of the bubble nose decreases the deviation between the numerical and analytical solution increases.
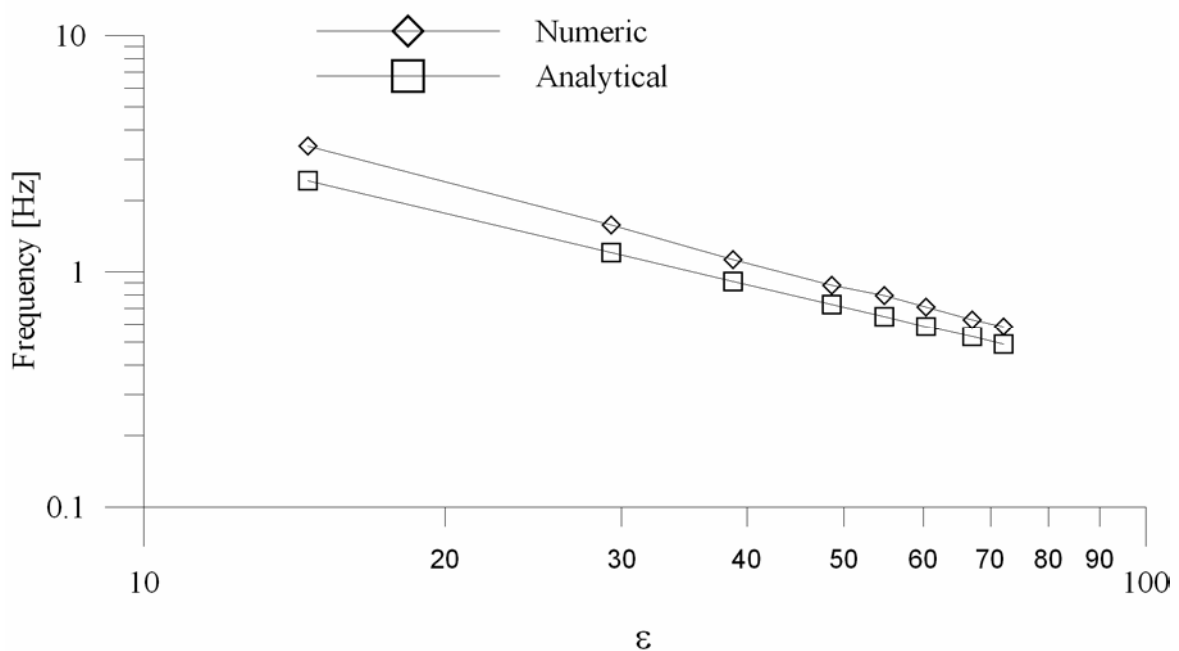

Figure 3 – Comparison between the numerical and analytical estimates of the natural frequency as a function of the parameter ε for the configuration defined on the test case.

A series of numerical simulations were performed changing pipe diameter, liquid velocity, bubble length, bubble void fraction, liquid slug length and discharge pressure to capture the influence of different parameters on the numerical determined natural frequency. The accuracy of the analytical expression is accessed comparing its output against the numerical solution as a function of the parameter ε defined in Eq. (28). Figure 4 shows the relative difference between the numerical and analytical results as a ε function. As expected, the relative difference on the natural frequency estimates decreases with ε increase. The relative difference can be as high as 35% at ε < 10. For ε > 50 the relative difference exhibits a bias of 17% with data scattered within ±10%. It is not clear at the moment the reason for the 17% bias between the numerical and analytical estimates even for values of ε →∞. On the other hand, the biggest relative differences are associated to ε < 10 and reflect the dominance of the non-linearity introduced by the H_1 coefficient from Eq. (21).
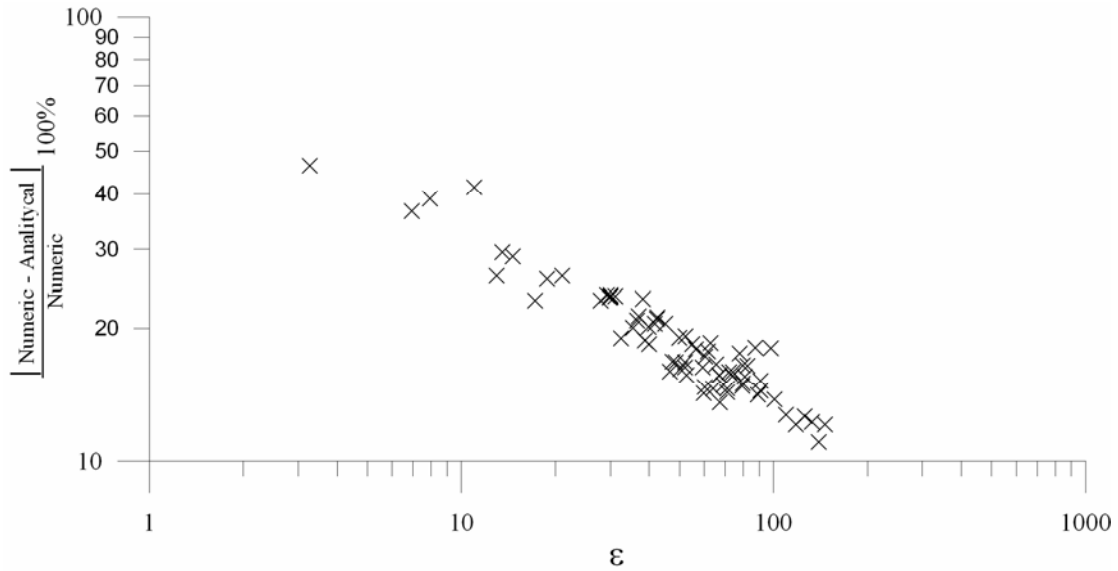
Figure 4 – Natural frequency relative difference as a function of parameter ε.

The accuracy of the analytical solution depends on the degree of 'linearity' of Eq.(14). It can be accessed drawing the solution trajectory on the phase plane $P_1 - U_1$. Figure 5 brings the numerical solution of P_1 and U_1 for the test case plotted on the phase plane. The equilibrium point have coordinates (P_1, U_1) of (100kPa, 0,5m/s). The trajectories are ellipses, centered at the equilibrium point, with semi-major and semi-minor axes very close to each other. If the semi-axes had the same sizes we would have circular trajectories which are representative of the linear system with $P1$ and U_1 described by Sin and Cos functions as shown by Eqs. (24) and (26). The lack of circularity on the trajectories is associated to degree of non-linearity of the system. The agreement of the analytical solution with the numerical one relies on the fact that the circular trajectories are good approximations to the elliptical trajectories.
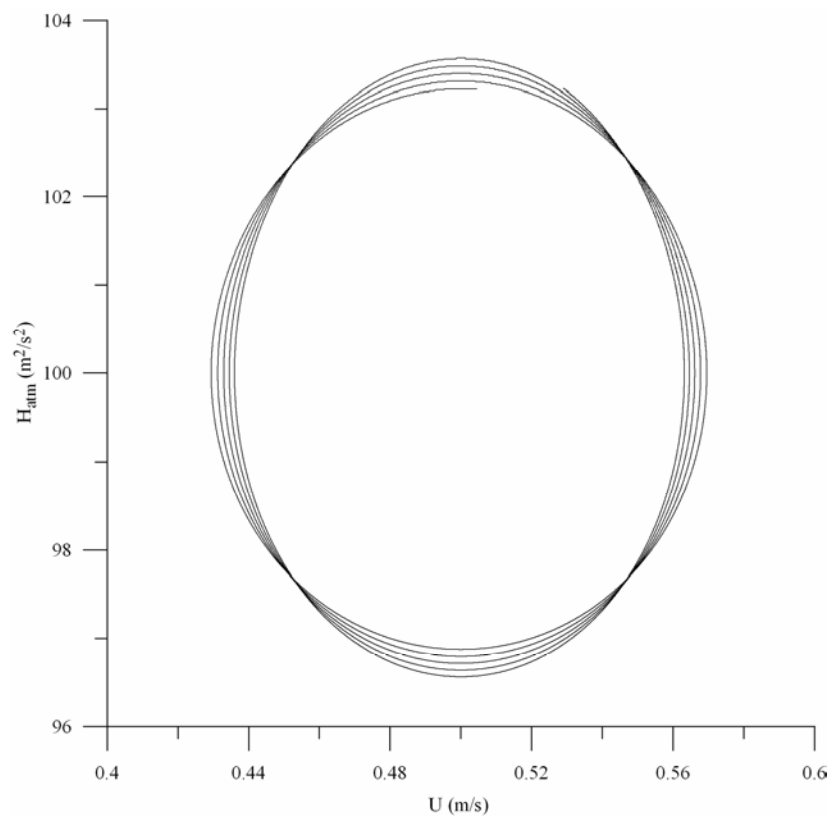

Figure 5 – Numerical solution trajectory on the phase plane P1-U1 for the test case.

4. CONCLUSIONS

A slug flow characterized by a single and long gas bubble flowing between two liquid slugs can be viewed as fluid non-linear oscillator. The system can be set to oscillate when a liquid velocity disturbance is introduced. The set of equations describing the bubble pressure and slug velocity can be linearized to render analytical solution. The analytical solution approaches asymptotically the numerical solution when the parameter ε increases. The bubble pressure and the liquid slug lag 90 degree in phase. The natural frequency of the single bubble oscillator is given by Eq. (25) within the linear approximation domain, i.e., $\varepsilon > 50$. It is proportional to the bubble pressure and inversely proportional to the product of: bubble length, slug length, liquid density and bubble void fraction.

5. ACKNOWLEDGEMENTS

6. REFERENCES

Bendiksen, K.H., 1984, "An Experimental Investigation of the Motion of Long Bubbles in Inclined Tubes", Int. J. Multiphase Flow, Vol. 10, pp. 467-483.

Franklin,, E.M., 2004, "Bubble Dynamics Segments Numeric Modeling in Horizontal Gas-liquid Intermittent Flow", MsC Dissertation, FEM/UNICAMP, Campinas, SP, Brazil, 235 p.

Grenier, P., 1997, "Evolution des longueurs de bounchons en écoulement intermittent horizontal", PhD Thesis, Institut de Mécanique des Fluides de Toulouse, Institut National Polytechnique de Toulouse, Toulouse, France, 193 p.

James, M.R., Lane, S.J., Chouet, B. and Gilbert, J.S., 2004, "Pressure Changes Associated with the ascent and bursting of gas slugs in liquid-filled vertical and inclined conduits", Journal of Volcanology and Geothermal Research, Vol. 129, pp. 61-82.

Leighton, T.G., 1994, "The acoustic Bubble", Academic Press, Londom, United Kindon, 613 p.

Liang, S.B. and Ma, H.B., 2004, "Oscillating Motions of Slug Flow in Capillary Tubes", Int. Comm. Heat Mass Transfer, Vol. 31, No. 3, pp. 365-373.

Nicklin, D.J., Wilkes, J.O. and Davidson, J.F., 1962, "Two Phase Flow in Vertical Tubes", Trans. Inst. Chem. Engineers, Vol. 40, pp. 61-68.

Swift, G., 2002, "Thermoacoustics: A unifying Perspective for Some Engines and Refrigerators", Acoustical Society of America, 320 p. < http://asa.aip.org/books/thermoacoustics.html>

Vergniolle, S. and Brandeis, G., 1996, "Strombolian explosions 1. A Large Bubble Breaking at the Surface of a Lava Column as a Source of Sound", Journal of Geophysical Reaserch, Vol. 101, No. B9, pp. 20,433-20,447.

Vergniolle, S., Brandeis, G. and Mareschal, J.C., 1996, "Strombolian explosions 2. Eruption Dynamics Determined form Acoustic Measurements", Journal of Geophysical Reaserch, Vol. 101, No. B9, pp. 20,449-20,466.

7. RESPONSIBILITY NOTICE

The authors are the only responsible for the printed material included in this paper.